



HAL
open science

GRACE Hydrological estimates for small basins: Evaluating processing approaches on the High Plains Aquifer, USA

Laurent Longuevergne, Bridget R. Scanlon, Clark R. Wilson

► **To cite this version:**

Laurent Longuevergne, Bridget R. Scanlon, Clark R. Wilson. GRACE Hydrological estimates for small basins: Evaluating processing approaches on the High Plains Aquifer, USA. *Water Resources Research*, 2010, 46, pp.11517. 10.1029/2009WR008564 . hal-00708088v1

HAL Id: hal-00708088

<https://hal.science/hal-00708088v1>

Submitted on 14 Jun 2012 (v1), last revised 14 Jun 2012 (v2)

HAL is a multi-disciplinary open access archive for the deposit and dissemination of scientific research documents, whether they are published or not. The documents may come from teaching and research institutions in France or abroad, or from public or private research centers.

L'archive ouverte pluridisciplinaire **HAL**, est destinée au dépôt et à la diffusion de documents scientifiques de niveau recherche, publiés ou non, émanant des établissements d'enseignement et de recherche français ou étrangers, des laboratoires publics ou privés.

GRACE Hydrological Estimates for Small Basins: evaluating processing approaches on the High Plains Aquifer, USA.

Laurent Longuevergne (1, 2), Bridget R. Scanlon (1), Clark R. Wilson (2)

5

(1) Bureau of Economic Geology, Jackson School of Geosciences, The University of Texas at Austin, 10100 Burnet Rd., Austin, TX, USA

(2) Department of Geological Sciences, Jackson School of Geosciences, The University of Texas at Austin, PO Box X, Austin, TX, USA

10

15

20

Submitted to:
Water Resources Research

25

Revision II
Revised manuscript

Corresponding author: laurent.longuevergne@beg.utexas.edu

30

Abstract

35 The Gravity Recovery and Climate Experiment (GRACE) satellites provide observations of water storage
variation at regional scales. However, when focusing on a region of interest, limited spatial resolution and noise
contamination can cause estimation bias and spatial leakage, problems that are exacerbated as the region of
interest approaches the GRACE resolution limit of a few hundred km. Reliable estimates of water storage
40 variations in small basins require compromises between competing needs for noise suppression and spatial
resolution. The objective of this study was to quantitatively investigate processing methods and their impacts
on bias, leakage, GRACE noise reduction, and estimated total error, allowing solution of the trade-offs. Among
the methods tested is a recently developed concentration algorithm called spatio-spectral localization, which
optimizes the basin shape description taking into account limited spatial resolution. This method is particularly
suited to retrieval of basin-scale water storage variations and is effective for small basins. To increase
45 confidence in derived methods, water storage variations were calculated for both CSR and GRGS GRACE
products, which employ different processing strategies. The processing techniques were tested on the
intensively monitored High Plains aquifer (450,000 km² area), where application of the appropriate optimal
processing method allowed retrieval of water storage variations over a portion of the aquifer as small as ~
200,000 km².

50

1.0 Introduction

The GRACE mission, launched in March 2002 [Tapley et al., 2004], has proven to be an excellent
complement to ground-based hydrologic measurements to monitor water mass storage variations within the
Earth's fluid envelopes. The dominant GRACE signal reflects changes in vertically integrated stored water,
55 including variations from snow pack, glaciated areas, surface water, soil moisture, and groundwater at all
depths. In this way, GRACE's data are distinctly different from other remote sensing satellites which are
typically limited to observations near the land surface. Extracting water storage variations of any single
component (e.g. groundwater) requires disaggregating the vertically integrated water storage signal, either by
making assumptions (e.g. neglecting snow or surface water contributions) or by using models or other
60 observations to estimate certain components, such as soil moisture.

Numerous studies have shown that GRACE-derived stored water variations compare favorably with
ground-based measurements and hydrological models at spatial scales of several hundred km and greater. As
reviewed by Ramillien et al. [2008], these studies provide confidence that GRACE can be used to monitor
hydrological systems and to improve hydrological modeling [Lettenmaier and Famiglietti, 2006; Güntner, 2008].
65 GRACE data have been applied to monitoring soil moisture and/or groundwater depletion from drought or
irrigation [Leblanc et al., 2009; Rodell et al., 2009, Tiwari et al., 2009] and to extract flux information from the
water balance equation, such as evapotranspiration [Rodell et al., 2004b, Ramillien et al., 2006] or river
discharge [Syed et al., 2008b]. GRACE data have also been integrated into the modeling process, e.g. for
validating global land-surface models [Ngo-duc et al., 2007], validating parameterization of land-surface
70 schemes [Niu et al., 2006, Han et al., 2009], and validating modifications of land-surface models [Niu et al.,
2009]. Finally, GRACE data have led to improved descriptions of water fluxes, via joint calibration of hydrologic
models and river discharge [Werth et al., 2009] or via assimilation into land-surface models [Zaitchik et al.,
2008]. Such applications of GRACE data require both robust and bias-free estimates of water storage change
and error estimates to appropriately weight the data [Güntner, 2008]. At the same time, interest in using
75 GRACE data is expanding to smaller basins (i.e. basin areas $\leq 250\,000$ km²) and improved data processing is
required to reliably estimate water storage variations at these smaller spatial scales.

The GRACE mission consists of two satellites at an altitude of ~450 km in an identical polar orbit, one trailing the other by ~200 km [Schmidt et al. 2008]. GRACE measures mass redistribution on the Earth by monitoring very precisely the distance between the two satellites and by tracking their positions via the GPS constellation. Changes in mass distribution (due to movement of water, air, and other sources) alter Earth's gravity field and changes the distance (range) and speed (range-rate) between the satellites. Changes in range of ~2 μm over the ~200 km separation are detectable. This yields a sensitivity to mass change equivalent to a ~1 cm thick disk of water at the land surface, with dimensions of a few hundred km or larger. Numerous studies have demonstrated that with this sensitivity, GRACE can contribute usefully to understanding total water storage changes in large basins with dimensions of many hundreds to thousands of km. However, as the spatial scale of interest approaches a few hundred km, GRACE data are more difficult to use. The goal of this study is to assess methods of estimating changes in water storage from GRACE data when the area of interest is near this resolution limit.

GRACE responds to all sources of mass redistribution near the Earth's surface. Thus, it is important to correct measured range-rate variations for well recognized influences, which include atmospheric mass redistribution, ocean mass redistribution due to currents and winds, ocean and solid Earth tides, and others. These mass redistributions are estimated from climate, ocean, and other models and the associated mass variations are known as 'dealiasing products', (Bettadpur [2007]). Since dealiasing products are imperfect, new data releases (currently Release 04) have been computed over time to take advantage of improvements in dealiasing elements (such as the ocean tide model). Each release involves reprocessing all the range-rate data since launch in 2002, usually leading to demonstrable improvements in quality. The residual range-rate signal (after removing dealiasing products and effects of the solid Earth gravity field) should be due largely to terrestrial water storage variations, including ice storage change in polar areas and other effects such as rebound of previously glaciated regions and earthquakes.

Two types of products have been developed from GRACE range-rate data. One is a spherical harmonic (SH) expansion of the gravity field, analogous to a Fourier series representation for spherical geometry. Dimensionless coefficients of the expansion (Stokes coefficients) are the standard GRACE Level 2 product used in this study. Several sets of Stokes coefficients, reflecting varying computational strategies, are available at the official data repository <http://podaac.jpl.nasa.gov/grace/> (CSR, GFZ, JPL), and more recently from additional sources such as DEOS <http://www.lr.tudelft.nl/live/pagina.jsp?id=6062b504-715e-4a22-9e87-ab2231914a4b&lang=en>, ITG <http://www.geod.uni-bonn.de/itg-grace03.html> or CNES/GRGS <http://bgi.cnes.fr:8110/geoid-variations/README.html>). A second type of GRACE product translates range-rate residuals directly into a global set of localized surface mass concentrations ('mascons'), omitting the direct use of spherical harmonics. Mascon solutions are not examined in this study but are compared with SH solutions in Klees et al. [2008].

Changes in Stokes coefficients from month to month allow computation of maps of spatial water mass variations \hat{S} [see e.g. Wahr et al. 1998, Chambers, 2006]. The limited range of SH Stokes coefficients (typically to degree and order 60) fundamentally limits spatial resolution. Furthermore, noise contamination generally increases with increasing degree and order; therefore, those coefficients most important for fine

115 spatial resolution are the most noisy. Thus, a compromise is needed to meet dual goals of noise suppression and maximum spatial resolution. A main point of this study is to examine various approaches to this compromise by finding combinations of available SH terms that are optimal by various measures.

2. Basin-scale studies and associated bias and leakage

120 Stokes coefficients, $C_{l,m}$ and $S_{l,m}$ relative to degree l and order m , are generally estimated up to degree and order $L_{\max}=60$. This limit fixes spatial resolution at about 300 km (in SH expansions, spatial resolution is typically reported as $\pi a/L_{\max}$, where a is Earth radius). However, additional filtering is required to suppress increasing noise with increasing SH degree, leading to spatial resolution somewhat less than 300 km. A SH expansion of GRACE water storage variations can be displayed as a global map of month-to-month apparent surface mass changes, but these cannot be simply interpreted pixel by pixel like traditional remote sensing
125 images. Instead, comparison with independent observations or models must be made at the same spatial resolution, by representing these observations as SH expansions with the same L_{\max} and then applying the same filtering used with the GRACE data. Comparisons have generally been conducted in continental-scale studies [e.g. Syed et al., 2008a]. Careful attention must be paid when estimating basin-scale water storage, as described in this section.

130 A surface mass change estimate for a space-limited region of interest R with area R_0 requires a basin function h (Figure 1b), which is defined as 1 inside R and 0 outside the basin, i.e.

$$h(X) = \begin{cases} 1 & \text{if } X \in R \\ 0 & \text{if } X \in \Omega - R \end{cases}$$

, where X is position on the Earth's surface $X=(\theta, \varphi)$ and Ω represents the entire Earth surface. If L_{\max} approaches infinity, the basin function approaches its ideal shape, but for finite L_{\max} it is only an approximation
135 to the exact $h(X)$. The GRACE water storage estimate \hat{S}_0 over the region of interest of area R_0 is then

$$\hat{S}_0 = \frac{1}{R_0} \int_{\Omega} \hat{S} h d\Omega \text{ [Wahr et al., 1998].}$$

A basin function can be described either on the Earth surface or in terms of SH coefficients $h(X) \rightarrow (h_{l,m}^C \text{ and } h_{l,m}^S)$; therefore, the estimate can also be written as a linear combination of the GRACE Stokes coefficients [Swenson et al., 2003]:

$$140 \quad \hat{S}_0 = \frac{4\pi a^3 \rho_e}{3R_0} \sum_{l=0}^{L_{\max}} \sum_{m=0}^l \frac{2l+1}{1+k'_l} (C_{l,m} h_{l,m}^C + S_{l,m} h_{l,m}^S)$$

where ρ_e represents the Earth's mean density. The weighting factor $\frac{2l+1}{1+k'_l}$ accounts for the Earth's response to surface mass loads at each SH degree, including both direct Newtonian attraction and elastic deformation via the load Love numbers k'_l , derived from seismic Earth models such as PREM [Dziewonski and Anderson, 1981] after solving gravito-elasticity equations [Pagiatakis, 1990; Guo et al., 2004].

Because water storage estimates can be expressed as a set of linear weights applied to the Stokes coefficients, these estimates can be developed with the goal of both maximizing resolution within the region of interest and filtering high degree and order Stokes coefficients to suppress noise (Figure 1b) [Swenson and Wahr, 2002]. The Effective Basin Function (EBF) \hat{h} is defined as the spatial function on the surface of the sphere and its corresponding SH weights applied to GRACE Stokes coefficients developed with these two goals in mind. \hat{h} describes the ability of GRACE to determine an average water storage change within the basin of interest. There is more than one way to select the EBF \hat{h} and a main goal of this study is to investigate how the EBF affects estimates of water storage variations.

In practice, SH truncation and filtering associated with \hat{h} modifies the basin shape. An example is shown in Figure 1b illustrating two differences relative to the exact basin function h . First, the mean value of the EBF over the basin of interest is no longer unity (which would lead to a biased estimate) and the EBF is not zero outside the basin, making the estimates sensitive to water storage changes outside the basin of interest (leakage). Bias and leakage time series may be calculated numerically considering the EBF \hat{h} [Klees et al. 2007]: $\bar{S}_0 = \hat{S}_0 + bias - leak$ where

$$bias = \frac{1}{R_0} \int_R S_0 (h - \hat{h}) d\Omega \quad (1) \text{ and}$$

$$leak = \frac{1}{R_0} \int_{\Omega - R} S_{leak} \hat{h} d\Omega \quad (2),$$

where S_0 is true stored water variation and \bar{S}_0 is average stored water over R . S_{leak} is true stored water variation outside the basin and \hat{S}_0 is the GRACE estimate before bias and leakage corrections. Note that terminology used here differs somewhat from other studies. For example, Wahr et al. [1998] and Swenson and Wahr [2002] consider 'leakage' to include effects of both bias (here associated with variations within the basin) and of variations external to the basin (Figure 1b).

Bias and leakage effects depend on actual water storage variations (both interior and exterior to the basin) and must generally be estimated from hydrological models. There is more than one way to select the EBF \hat{h} and a main goal of this study is to investigate how the EBF affects estimates of water storage variations. The quality of the EBF may be measured by concentration near unity (ability to describe the area of interest) and rejection of contributions from surrounding areas (i.e. reducing leakage effects). EBF concentration is defined as

$$\Lambda = \int_R \hat{h}^2 d\Omega / \int_{\Omega} \hat{h}^2 d\Omega \quad (3),$$

the integrated squared value within the basin of interest relative to the globally integrated squared value. For example, a concentration of 0.9 means that only 10% of the variance (energy) originates from outside of the region of interest.

[FIGURE 1]

180 Chen et al. [2005] showed that bias can generally be corrected to within a few percent using a simple multiplicative factor to rescale GRACE water storage estimates assuming a uniform distribution of water over the basin and no water storage variation outside the basin. The multiplicative factor k is then

$$k = \left(\frac{1}{R_0} \int_R \hat{h} d\Omega \right)^{-1} \quad (4)$$

185 Fenoglio-Marc et al. 2006, Velicogna and Wahr, 2006, Swenson and Wahr, 2007]. A second approach to determine bias and leakage employs a hydrological model. From the model, an equivalent rescaling factor is calculated as the ratio of hydrological model water storage mean value over a basin to values determined from the basin region after truncation and filtering of GRACE Stokes coefficients. Chen et al., [2007] show that the hydrological model does not need to be precise to allow accurate determination of this multiplicative factor.

190 Leakage arises from hydrological conditions outside the basin and is not generally described by a single multiplicative factor. Bias and leakage correction methods are summarized in Table 1, highlighting the different assumptions. Rodell et al. [2009] emphasize the importance of adapting bias and leakage estimation methods to a particular basin and estimated water storage variation. Recently, Baur et al. [2009] proposed an iterative process using forward modeling to correct for both leakage and bias.

195 [TABLE 1]

If temporal water storage variations are spatially homogeneous over a large area, bias and leakage partially cancel one another and filtered GRACE solutions may agree quite well with unfiltered estimates of water storage from hydrological models [Chen et al., 2005]. Leakage effects tend to be reduced for basins near oceans where storage variations are generally smaller, with the result that the bias effect may cause filtered GRACE data to significantly underestimate water storage variations in the basin. Additional leakage problems have been observed for adjacent basins whose storage changes are out of phase (for example, the Orinoco and Amazon basins).

205 [FIGURE 2]

The different processing steps to estimate GRACE water storage variations at basin-scale are synthesized in Figure 2. There were two main objectives in this study. The first (Section 3) was to survey methods for estimating water storage variations considering problems of bias, leakage, and GRACE error, especially for basins with spatial dimensions near the limit of GRACE resolution, between about 450 and 750 km and to determine the best concentration/filtering method that minimizes GRACE error and leakage correction error. A number of previously published approaches were surveyed and compared with an optimal concentration method based on spatio-spectral localization [Simons et al., 2006]. The second objective (Section 4) was to

215 derive and then apply the best suited method minimizing both GRACE error and leakage correction error for
the particular case of the High Plains Aquifer (HPA) in central North America (Figure 1), a major groundwater
resource. The HPA provides an interesting and useful test case to evaluate methodologies because of its size,
irregular shape, and availability of detailed surface and groundwater monitoring. To supplement in situ
observations, leakage effects were quantified using a numerical data assimilating water storage model. Results
220 from this study are important for testing applicability of GRACE to other areas of similar size and irregularity in
shape.

3.0 Filtering and Construction of the Effective Basin Function

Construction of GRACE changes in water storage typically involves two steps. The first is to filter GRACE
data to suppress noisy high degree and order SH coefficients, and the second is to find an effective basin
225 function \hat{h} best concentrated within the region of interest considering a limited range of SH. These steps are
treated separately in this study, although they are not completely independent. Filtering impacts concentration
by removing signal at high degrees and orders, as shown by Chen et al. [2007], and concentration may
improve the signal to noise ratio by limiting noise leakage into the region of interest [Han et al., 2008]. The
quest to find the optimal filtering and concentration methods depends on the nature of the noise, size and
230 shape of the region of interest, and, to some extent, the hydrological setting of the region. Therefore, solutions
need to be tailored to the region of interest. Three parameters are listed to measure the quality of an EBF. The
first two depend only on geometrical properties of the region of interest:

- the EBF concentration Λ
- $b=k^{-1}$, the mean value of the EBF over the region of interest (the reciprocal bias).

235 The third parameter measures the efficiency of investigated methods: the final error $\Delta\bar{S}_0$ on GRACE basin-
scale water storage estimate, after bias and leakage corrections.

3.1 Filtering to Suppress GRACE Measurement Noise

Two types of filters for suppression of noisy SH coefficients are in general use: (1) fixed parameter
filters and (2) data adaptive filters (i.e. filters that adjust their transfer functions according to an optimizing
240 algorithm). Fixed parameter filters include isotropic Gaussian (applied equally to all orders at each degree)
[Jekeli et al., 1981; Wahr et al., 1998] and cosine taper or anisotropic filters [Wooters et al., 2007]. Data-
adaptive filters may use geophysical models or GRACE observations to judge noise and signal levels. These
may be isotropic or anisotropic [Guo et al., 2009, Han et al., 2005; Sasgen et al., 2006; Seo et al., 2006;
Swenson and Wahr, 2006; Kusche, 2007]. Additional examples include the adaptive filter of Klees et al. [2008]
245 which minimizes root mean square error (rmse) while accounting for signal variance and covariance and the
iterative least squares filter to pass signal and reject noise, using a-priori water storage estimates from
hydrological models [Ramillien et al, 2005].

Besides suppression of noisy high degree Stokes coefficients, another important problem is
suppression of longitudinal stripes found in most current GRACE solutions. These stripes are due to the ill-

250 posed nature of the least squares estimation problem [Save, 2009] and to aliasing of geophysical signals at
 timescales below one month [Seo et al., 2008]. Swenson and Wahr [2006] developed an effective data-
 adaptive polynomial filter to remove the stripes. It is possible that future GRACE product releases will suppress
 these stripes. A modified version of the Swenson and Wahr [2006] destriping filter was applied in this study. A
 4th degree polynomial was fit for SH orders 6 to 40. Above SH degree 40, the polynomial degree was reduced
 255 to 3 up to degree 50.

The performance of the following common fixed-parameter filters was examined

- An isotropic Gaussian filter, expressed by coefficients W_l for all orders of spherical harmonics of degree l

$$W_l = \exp\left(-\frac{(lr)^2}{4\ln(2)a^2}\right)$$

260 where r is the half-length radius of the filter (Figure 3). Sasgen et al. (2006) showed that the optimal isotropic
 Wiener filter is close to a Gaussian filter with a 400 km half radius.

- An isotropic cosine taper, also defined in the SH domain by

$$W_l = \begin{cases} 1 & \text{if } l < l_1 \\ \frac{1}{2} \left(1 + \cos\left(\pi \frac{l-l_1}{l_2-l_1}\right) \right) & \text{if } l_1 < l < l_2 \\ 0 & \text{if } l > l_2 \end{cases}$$

(Figure 3). The half-length wavelength is defined as $\frac{2\pi a}{(l_1+l_2)}$. The cosine taper has the advantage of

265 suppressing only the highest SH degrees, leaving mid degrees unchanged. The bandwidth is also better
 limited, suppressing entirely SH degrees above l_2 .

[FIGURE 3]

270 **3.2 Construction of the Effective Basin Function**

The purpose of EBFs is to best describe the area of interest considering the maximum degree L_{\max} of
 GRACE products. No EBF can be strictly both space-limited and band-limited to a range of SH coefficients
 below L_{\max} [Percival and Walden, 1993]. While space-limited methods may be seen as most adapted to
 examine specific regions of interest, truncation of the SH expansion to degree 60 affects their shape (Figure
 275 1b). Methods that work directly with the SH coefficients are thus more suited to investigate water mass
 variations from GRACE associated with a localized geophysical phenomenon because they allow control over
 the useful range of Stokes coefficients.

The simplest approach to the concentration problem is to truncate the exact basin function to the range of
 available spherical harmonics. An east-west section through a simple truncated basin function ($L_{\max}=60$) is
 280 shown in Figure 1b, along with related statistics concerning bias and leakage. Simple truncation produces large
 oscillating sidelobes outside the region of interest. Two modifications to this approach were also examined in

285 this study. The first modification is to use a truncated function with the smallest convex region containing the basin of interest, as indicated in Figure 1a. The Matlab “convhull” function was used to select from the original contour the contour points describing the smallest convex shape. This simple geometric operation leads to smoothing of complicated basin shapes and increases the amplitude of low and mid SH degrees relative to simple truncation. The second modification is to use a Hamming Window instead of sharp truncation of Stokes coefficients. This reduces sidelobes outside the region of interest. Simple truncation and the two modifications depend entirely on the geometry of the region of interest.

290 A data-adaptive method developed by Swenson et al. [2003] aims at minimizing the sum of GRACE error and leakage error. This method is neither space-limited nor band-limited (except if GRACE errors are considered as infinite for $l \geq L_{\max}$) but it has the important characteristic of damping noisier high degree SH’s.

The isotropic modification of the basin function leads to $\hat{h}_{lm} = \left(1 + \frac{2B_l^2}{(2l+1)\sigma_0^2 G_l}\right)^{-1} h_{lm}$, where, B_l are degree amplitudes of GRACE measurement errors given in terms of an equivalent water layer, G_l are Legendre coefficients of an assumed exponentially decaying signal spatial covariance function, and σ_0^2 is signal variance. This EBF is generally insensitive to the correlation length of the signal covariance function, and a value of 500-km was used in this study, in the mid-range of that suggested by Swenson et al. [2003]. This is referred to as Swenson’s EBF in the following. GRACE error is taken as the formal error provided by GRACE processing centers. Because formal error likely underestimates true error, Swenson’s window is used in combination with other filters that suppress high SH coefficients. This window would perform optimally using realistic error estimates, which are not necessarily reported with GRACE products from the various processing centers

300 Recently, new methods for SH analysis, called spatio-spectral localization, have been developed to maximize the concentration parameter Λ [Simons and Dahlen, 2008]. This work follows from Fourier time series analysis results from Slepian [1978] leading to multitaper spectral analysis methods [Thomson, 1982]. The idea is to find, for maximum SH degree L_h , functions that maximize the concentration Λ from equation (3). Wieczorek and Simons [2005] derived this result for axi-symmetric windows and it was extended to arbitrary domains by Simons et al. [2006]. There is a set of functions \hat{h} that maximize Λ , all are eigenvectors of the eigenvalue problem $D\hat{h} = \lambda\hat{h}$, where matrix D contains integrals of products of Legendre polynomials.

310 The resulting set of Slepian functions \hat{h} are orthogonal over both the entire sphere and on the region of interest. Among the $(L_h + 1)^2$ solutions to this equation, only well-concentrated solutions ($\lambda \approx 1$) are used. The number N of well-concentrated solutions \hat{h} is found from the equivalent of the Shannon number on a sphere,

$$N = (L_h + 1)^2 \frac{R_0}{4\pi a^2},$$

which is the product of the SH bandwidth and the normalized area of the basin of interest

[Simons et al., 2006]. L_h may be chosen to be as large as L_{\max} . However, in practice, L_h is maintained as small as permitted by the size of the basin. The goal is to achieve a balance between spatial and spectral

315 concentration [Dahlen and Simons, 2008] and to limit noise contamination from GRACE high-degree SH
 coefficients. The final EBF is built as the sum of the chosen N well-concentrated \hat{h} .

3.3 GRACE Noise Levels

Numerous studies of GRACE errors have been published. Wahr et al. [2004] and Seo et al. [2006] provide
 320 overviews of the GRACE error budget in water storage estimates using GRACE Release 1 (RL01) solutions.
 For a given month, RMSE values are typically in the range of 5 mm (equivalent water thickness) for the
 fundamental GRACE measurement (satellite to satellite range-rate) and 10 to 50 mm for errors in atmospheric
 and oceanic corrections depending on latitude. GRACE measurements tend to be more precise at high-
 latitudes due to increased track density associated with a polar orbit, but atmospheric and oceanic dealiasing
 products typically degrade in quality at higher latitudes [Seo et al., 2005]. Wahr et al. [2006] proposed an
 325 estimate of error from non-seasonal GRACE residuals over land, after subtracting annual and semi-annual
 sinusoids and smoothing, but this approach tends to overestimate errors when there are significant
 nonseasonal signals. Chen et al. [2009] estimated errors from residual variations over the oceans taking into
 account atmospheric effects not in dealiasing products. Deficiencies in oceanic dealiasing products might
 cause this error estimate to be too large as well. However, both error estimates are similar, with RMSE values
 330 about 25 mm (equivalent water layer thickness) depending on the latitude of the basin.

Concentration effects (i.e. bias and leakage correction errors) should also be considered when focusing on
 a space-limited area. In the following, bias is assumed to be corrected using the multiplicative factor k , which
 implies spatially homogeneous variations within the basin. For simplicity in estimating leakage correction error,
 mass variations outside the area of interest are also considered as spatially homogeneous with amplitude S_{leak}

335 in the region of sensitivity of the EBF. Leakage can then be rewritten as $leak = \beta S_{leak}$ with $\beta = \int_{\Omega-R} \hat{h} d\sigma$. Finally,

the total error $\Delta \bar{S}_0$ may be written as $\Delta \bar{S}_0 = k \Delta \hat{S}_0 + \hat{S}_0 \Delta k + \Delta(k\beta) S_{leak} + k\beta \Delta S_{leak}$.

Total error is the sum of:

- $k \Delta \hat{S}_0$, level-2 GRACE error estimate, amplified by bias correction. The methodology of Chen
 et al. (2009) was used in this study to estimate $\Delta \hat{S}_0$. RMS variability was calculated over all
 340 oceans in a latitudinal band containing the basin, but excluding ocean regions within 1000 km
 of continents to avoid leakage from terrestrial storage changes. Over an area equivalent to the
 High Plains aquifer, the error $\Delta \hat{S}_0$ is on the order of 10 mm using a 300-km Gaussian
 smoother for GRACE data measured after 2002.
- $\Delta k \hat{S}_0 + \Delta(k\beta) S_{leak}$ is the calculation error in estimating bias and leakage effects. It includes
 345 both numeric errors in integral calculation and error in approximating the basin using
 rectangular grids. With 0.25 degree grid resolution this error is < 1% (figure 4) and with 0.5

degree grid this error is < 2%. A similar grid for a hydrological model would accurately correct leakage effects.

350

[FIGURE 4]

- $k\beta \Delta S_{leak}$ is the error due to leakage correction, which is derived from a hydrological model and linked to the concentration parameter. This error is difficult to evaluate because it requires an error estimate from an a-priori hydrological model. As a first guess, a standard deviation from differences among VIC, MOSAIC, CLM, and NOAH land surface models, included in GLDAS [Rodell et al., 2004], was used. Unfortunately, all models in GLDAS use the same forcing dataset; therefore, errors are probably correlated and resulting value of 30 mm may thus be an underestimate.

355

4. Application to the High Plains Aquifer

360

The unconfined High Plains aquifer (HPA) (450,000 km² area, Figure 1a) is the principal source of water for one of the major agricultural areas in the world in central North America. The climate of the region is mostly semiarid, with mean annual precipitation (P) ranging from 350 mm in the west to 750 mm in the east and mean annual temperature from 7.5°C in the north to 18°C in the south (PRISM mean 1895 – 2008, www.prismoregonstate, Daly et al., 2008, DiLuzio et al., 2008). Potential evapotranspiration greatly exceeds precipitation; therefore, agriculture in the region is heavily dependent on irrigation, mainly from groundwater. The HPA was specifically mentioned in the National Research Council report “Satellite Gravity and the Geosphere” as suitable for study with a satellite system like GRACE [Dickey et al., 1997] and a prelaunch study by Rodell and Famiglietti [2002] confirmed this. Since then, Strassberg et al. [2007, 2009] verified that GRACE can monitor HPA water storage variations, showing that at seasonal time-scales, GRACE data agree well with water storage estimates from ground-based measurements.

365

370

4.1 Data and Processing

375

Two different GRACE data sets were used to test the filtering and concentration schemes examined in this study. The first is monthly samples from the Center for Space Research (CSR) RL04 GRACE SH ($L_{max}=60$) [Bettadpur, 2007]. The second is 10-day samples produced by CNES-GRGS (Groupement de Recherche en Géodesie Spatiale) RL01 ($L_{max}=50$) [Lemoine et al., 2007]. GRGS solutions are stabilized so that the time-variable part of the Stokes coefficients diminish to 0 at degree 50. CSR and GRGS solutions use the same range-rate data and similar geophysical models, but employ independent processing strategies. Therefore, it is interesting to compare results for the HPA using both.

380

In all cases, total water storage variations from GLDAS NOAH [Rodell et al., 2004], available on a 0.25 degree grid, was taken as the a-priori hydrological model to correct for leakage effects. GRACE mass storage estimates were compared to GLDAS-NOAH predictions (monthly or 10-day averages) and to water storage variations derived from groundwater table elevations and soil moisture point measurements and analyzed by

385 Strassberg et al. [2009]. The soil moisture and groundwater data were also analyzed at a daily time step using the Karhunen-Loeve transform to extract significant modes of spatial and temporal variability from the point measurements. Kriging was then performed on the spatial pattern associated with each mode to calculate a spatial mean. The details of this modal upscaling analysis are beyond the scope of this paper and can be found in Longuevergne et al. [2007]. The resulting time-series is, however, given as an alternative to that of Strassberg et al. [2009]. They calculated mean soil moisture variations over a 1 degree grid when data were available. A seasonal signal was assumed to calculate groundwater storage variations and determined using available data. Differences between the two estimates provide a measure of uncertainty in water storage estimates derived from the point measurements. At monthly time-scales, the variance of the mode-derived time series is reduced relative to that of Strassberg et al. [2009] by 8% and the correlation between the two analyses is 0.92.

395 **4.2 Comparison of Concentration Methods**

395 Five different EBFs have been used to estimate HPA water storage variations from GRACE (Figure 5). In the case of the Slepian EBF, the maximum degree and order was set at $L_h=50$ and the first two solutions to the eigenvalue problem $D\hat{h}=\lambda\hat{h}$ are used to describe the elongated shape of the HPA. Experimentation with a large value $L_h=60$ (a possibility with the CSR solution) would allow computing an EBF based on the first three solutions and better describe the shape of the HPA. However, this choice did not significantly improve concentration and reciprocal bias; therefore, using the full range of Stokes coefficients available with the CSR solution would not be optimal in terms of final error.

400 Leakage problems are illustrated after rescaling the EBF to restore the signal amplitude (Figure 5a). Sidelobe oscillations are partially damped by Gaussian filtering. Other methods besides the truncated basin function, including the convex truncated basin function, are less subject to oscillation problems. When a filter is applied, the EBFs converge more quickly towards 0 outside the area of interest.

405 The difference between the EBF \hat{h} and the true basin h was used to evaluate bias and leakage effects (Figures 5 b and c). The fact that the EBF is not homogeneous over the entire region of interest should be taken into account, especially for irregularly-shaped basins such as the HPA.

410

[FIGURE 5]

415 The five EBFs have different characteristics affecting the SH spectrum of the solution (Figure 6). Swenson's EBF damps the highest degree coefficients to reduce Stokes coefficient errors that increase with degree. In contrast, the convex function amplifies the highest degrees and diminishes the lowest degrees (Figure 6c). Because the Slepian EBF is derived by an optimization process, it is not simply related to the exact basin function. At low degrees EBFs are identical but at higher degrees, specific degrees and orders are amplified or damped (Figure 6b).

420 After windowing by the original basin function, the GLDAS spectrum diminishes slowly as SH degree increases (Figure 6c) but GRACE error limits the ability to recover these high degrees. Swenson's EBF, which uses the GRACE formal error spectrum, is likely the most effective in accounting for this. The Slepian EBF offers a trade-off among the EBFs, retaining mid-degrees to describe the basin shape while diminishing rapidly at higher degrees.

425 [FIGURE 6]

Leakage correction requires knowledge of the signal exterior to the basin and was estimated based upon GLDAS-NOAH stored water variations (considering snow, vegetation, and soil moisture) for various EBFs (Figure 7). Swenson's EBF and Slepian EBF reduce leakage below 15 mm most of the time. Leakage is also
430 dependent on the filtering method.

[FIGURE 7]

Bias was computed using both GLDAS-NOAH as a-priori information for true water storage inside the area of interest and the geometric multiplicative factor k . GLDAS-NOAH derived bias may then be expressed
435 as an equivalent multiplicative factor by a least-square fit to uncorrected GRACE data (Table 1). Both estimates may differ by up to 40%. Indeed, GLDAS-NOAH does not model groundwater storage variations and; therefore, significantly underestimates true water storage changes inside the HPA. For this reason, the SH approach described above was used to estimate the bias factor k

440 **4.3 Noise-Reduction – Spatial Resolution Trade-off**

Error in GRACE water storage estimates is linked to both the EBF properties and to the filtering method. An unfiltered EBF may exhibit excellent concentration, but in combination with filtering, concentration is diminished with resulting increases in bias and leakage (Figure 7a and b). The destriping filter may have a large impact because this filter removes variance similar in shape to the HPA, which trends north-south.
445 However, the real impact of the destriping filter is difficult to determine accurately. The destriping filter is data-adaptive (i.e. not a conventional linear filter) and fitted to GRACE data directly; therefore, predicting its effect cannot be undertaken by destriping the shape of the aquifer or results from hydrological models. In practice, as shown in table 2 and Figure 9, the amplitude of CSR time series is very close to that of the GRGS time series (which does not require any destriping) and to that of ground data. Therefore, destriping is assumed to have
450 little effect on concentration and bias in the following analysis. GRACE error without destriping is as high as 50 mm most of the time, whereas use of the destriping filter reduces GRACE error by a factor of ~ 10 (not shown on Figure 7c). This filter is thus absolutely necessary for CSR RL4 solutions. A cosine taper filter is an interesting alternative to the Gaussian filter and reduces leakage problems by filtering the highest degrees only and leaving mid degrees unchanged. It also has better spectral characteristics than the Gaussian filter.

455 Compared to a truncated basin function, the convex basin function decreases bias, showing that this
simple geometric operation can be useful for smaller basins. However, it does not perform well for the HPA
because of the indented shape of the HPA (its boundary is in places concave). Concentration is diminished as
a result, leading to larger leakage. However, the leakage is more concentrated near the edge of the HPA
460 compared to a simple truncated EBF. The Hamming EBF is generally inferior relative to the truncated or
convex EBF. Swenson's EBF performs very well providing high concentration despite the complicated shape of
the HPA.

For the CSR solution, the best combined concentration / filtering method is the Slepian EBF, supplemented
by a cosine taper between degrees 30 and 50 which results in a final RMSE of ~ 25 mm. When using a 300-km
Gaussian filter, GRACE error is higher (10 mm vs 7 mm); however, the leakage correction error is lower (~ 14
465 mm vs 18 mm). The optimum concentration / filtering method for the GRGS solutions is quite different because
GRGS solutions are stabilized. Because of the lack of stripes in GRGS solutions, in contrast to CSR solutions,
no additional filtering is optimum. Despite the GRGS $L_{\max} = 50$, GRACE error is higher (15 mm) but leakage
correction error is reduced to 12 mm. The final chosen filtering / concentration methods are described in table
1.

470 When using the CSR solution for the HPA, the choice of filtering method to reduce noise is more critical
than the concentration method. Most of the concentration methods lead to errors within 5 mm of one another.
In contrast, the concentration method was more important for the GRGS solution, which does not require
additional filtering for the HPA.

Deriving basin-scale water storage estimates using a truncated EBF does not lead to error estimates that
475 are significantly higher. However, the sensitivity of truncated EBFs to external masses may extend quite a
distance from the region (Figure 7), which is not properly translated here in the leakage correction error
estimate. As a result, leakage correction errors may be underestimated, especially in the case of large spatial
variations in water storage (e.g. in monsoon areas). In the latter cases, the use of Slepian window, by
maximizing concentration, would minimize sensitivity to water masses outside the area of interest and thus
480 leakage error.

GRACE error for deriving total water storage variations in both saturated and unsaturated zones is slightly
lower than the GLDAS-NOAH estimated error which is limited to soil moisture variations. GRACE thus provides
meaningful data to improve knowledge of the water cycle over the HPA and to recover groundwater storage
variations.

485

[FIGURE 8]

4.4 Water Storage Variations in the High Plains Aquifer

The optimal combination of concentration/filtering was applied to extract stored water variations for the
490 HPA. The selected processing scheme and the main characteristics are summarized in Table 1.

[TABLE 2]

495 CSR and GRGS solutions employ independent processing strategies and require different processing
methods, but GRACE water storage estimates agree well (Figure 9), which provides confidence in the
methodology and processing choices selected.

[FIGURE 9]

500

[TABLE 3]

505 Agreement between ground based total water storage estimates and GRACE estimates is generally very
good, except for the April 2003 peak. Correlations are ≥ 0.8 for CSR, at monthly and seasonal time-scales and
 ≥ 0.70 for GRGS solutions at 10-day time scales (Table 2). Although HPA is large, discharge from irrigation
and evapotranspiration and recharge from precipitation are far from uniform over the HPA, making spatial
resolution a challenging issue. Moreover, the EBFs for the HPA as a whole are not homogeneous because of
differential hydrological behavior and the elongated shape of the aquifer (Figure 6 b and c); therefore, division
into subregions should conform better to the homogeneity hypothesis assumed when using a simple scalar
bias correction k . To test this idea, the aquifer has been subdivided into a northern part (210,000 km²) and a
510 southern part (240,000 km²) by the 40th parallel. The northern and southern parts of the aquifer behave
differently. For example, the 100 mm recharge event during Sept-Oct, 2004 is restricted to the southern part of
the aquifer (Figure 9). Correlation with GRACE estimates is retained for the sub-basin time series, which
validates the concept of using GRACE to study regions at this scale. Note that the optimal filter for CSR
solutions differs for the northern and southern part of the aquifer.

515 GRGS 10-day solutions provide improved monitoring of rapid water storage variations, such as those
related to aquifer pumping during spring 2003 and spring 2006. Even if the correlation between GRACE and
ground-based measurements is slightly lower compared to monthly sampling, its value (≥ 0.70) at 10-day time
scales indicates that interesting information is available at shorter time scales than provided by the CSR
solutions.

520 In all cases, variance in GRACE water storage estimates exceeds that of ground-based water storage by
10 to 18 %. There are several potential explanations for this, including (1) overestimation of bias corrections
using the simple multiplicative factor k , (2) underestimation of leakage corrections related to underestimation
associated with the GLDAS-NOAH water storage estimates, and (3) inadequate ground measurements
producing biased regional estimates. Strassberg et al. (2009) found closer agreement between GRACE and
525 surface estimates with GRACE – variance exceeding ground-based variance by 5 to 10 %.

5. Summary

This study investigated how different processing choices may affect GRACE level-2 estimates of water
storage variations, considering problems of bias, leakage, and GRACE error when focusing on spatial scales

530 near the limit of GRACE resolution, between about 450 and 750 km. Leakage correction in particular relies on
an a-priori hydrological model; therefore, leakage should be reduced to make GRACE water storage variations
independent from a-priori hydrological models. Spatospectral concentration was introduced to minimize
leakage effects. This method allows restriction of the spherical harmonic bandwidth to achieve a balance
between spatial and spectral concentration, optimally describing the shape of the basin while avoiding noise
contamination from noisy high degrees Stokes coefficients. Reliable estimates of water storage variations
535 require a trade-off among GRACE noise reduction, maximum spatial resolution, and minimum spatial leakage,
achieved by minimizing errors related to GRACE and leakage correction. Optimum filter type and concentration
methods may vary from basin to basin, depending on geographical location, shape, characteristics of
hydrological signals in and surrounding the basin, and also GRACE noise characteristics. As a result, the
optimized method varies from region to region and should be determined separately for each basin and the
540 particular GRACE solution.

To increase confidence in derived methods, water storage variations are calculated for both CSR and
GRGS solutions, which employ different processing strategies. The approach to developing a processing
scheme in this study was validated for the High Plains Aquifer, where intensive monitoring of soil moisture and
groundwater has been conducted. Using the CSR GRACE solution for small basins, the choice of filtering
545 method is more critical than the concentration method. In contrast, the concentration method was more
important for the GRGS solution, which does not require additional filtering in this case. In both cases, Slepian
window was found to be the most suitable method for deriving estimates of water storage variations from
GRACE in a space-limited area. These windows are indeed optimized to reduce leakage effects, considering a
limited range of Stokes coefficients. The final error is ~ 25 mm, demonstrating the ability of GRACE to improve
550 knowledge of the water cycle over the HPA and to recover groundwater storage variations using appropriate
methods.

With suitable concentration and filter methods, it is possible to divide the High Plains Aquifer into two sub-
regions, demonstrating that GRACE can be used effectively with basins as small as $\sim 200,000$ km², with
irregular shapes. The shorter 10-day temporal sampling of GRGS solution also appears to provide useful
555 monitoring of rapid water storage variations, such as those related to groundwater pumping.

An important lesson from this study is dependence on oceanic and atmospheric models, as well as data
assimilating land surface models like GLDAS to optimize the use of GRACE data. While a goal of the GRACE
mission is to provide independent measures of the water cycle, it is clear, especially for smaller basins, that an
iterative analysis will be most effective. In all future gravity measurements from space, it is anticipated that land
560 surface models will continue to guide formulation of GRACE water storage variation estimates, as, in turn,
GRACE or other gravity satellite estimates contribute to land surface models.

Acknowledgment

Funding for this study was provided by NASA (grant NNX08AJ84G) and the Jackson School of Geosciences at
the University of Texas at Austin. We feel grateful to Harihar Rajaram, Tissa Illangasekare as well as the 3
565 anonymous reviewers to help improving the manuscript. The authors would like to thank Maggie Dunklee from

USGS-SCAN, Wes Burgett from the West Texas Mesonet, Jeffrey Basara from the Oklahoma Mesonet, Nathalie Umphlett from the High Plains Regional Climate Center, the Atmospheric Radiation Measurement Program, and David Wedin for making available soil moisture measurements for this study. The authors thank Frederik Simon for fruitful discussion on spatio-spectral localization. His computer algorithms are available on www.frederik.net. Computational resources were provided by Effie Jarrett (DGS, UT Austin). The authors would like to thank Gil Strassberg for his assistance and advices.

6. References

- Baur, O., M. Kuhn, and W. E. Featherstone (2009), GRACE-derived ice-mass variations over Greenland by accounting for leakage effects, *J. Geophys. Res.*, 114, B06407, doi:10.1029/2008JB006239.
- Bettadpur, S (2007). Level-2 Gravity Field Product User Handbook, GRACE 327-734, The GRACE Project, Center for Space Research, University of Texas at Austin.
- Chambers, D.P. (2006). Evaluation of New GRACE Time-Variable Gravity Data over the Ocean. *Geophys. Res. Lett.*, 33(17), L17603
- Chen, J. L., C. R. Wilson, J. S. Famiglietti, and M. Rodell (2005). Spatial sensitivity of the Gravity Recovery and Climate Experiment GRACE time-variable gravity observations, *J. Geophys. Res.*, 110, B08408, doi:10.1029/2004JB003536.
- Chen, J. L., C. R. Wilson, J. S. Famiglietti and M. Rodell (2007). Attenuation effect on seasonal basin-scale water storage change from GRACE time-variable gravity, *J. Geodesy*, 81, 237–245.
- Chen, J.L., C.R. Wilson, B.D. Tapley, Z.L. Yang and G.Y. Niu (2009). 2005 drought event in the Amazon River basin as measured by GRACE and estimated by climate models, *J. Geophys. Res.*, 114, B05404, doi:10.1029/2008JB006056.
- Dahlen, F. A. and F. J. Simons (2008). Spectral estimation on a sphere in geophysics and cosmology. *Geophys. J. Int.*, 174, 774–807. doi:10.1111/j.1365-246X.2008.03854.x
- Daly, C., M. Halbleib, J.I. Smith, W.P. Gibson, M.K. Doggett, G.H. Taylor, J. Curtis and P.A. Pasteris (2008). Physiographically-sensitive mapping of temperature and precipitation across the conterminous United States. *International Journal of Climatology*, DOI: 10.1002/joc.1688.
- DiLuzio, M., G.L. Johnson, C. Daly, J.K. Eischeid and J.G. Arnold (2008). Constructing retrospective gridded daily precipitation and temperature datasets for the conterminous United States. *Journal of Applied Meteorology and Climatology*, 47: 475-497
- Dickey, J.O and the National Research Council Committee on Earth Gravity from Space (1997). *Satellite Gravity and the Geosphere. : Contributions to the Study of the Solid Earth and Its Fluid Envelope*, Natl. Acad., Washington, D. C.
- Dziewonski, A. and D. Anderson, (1981). Preliminary reference earth model, *Phys. Earth planet Inter.*, 25, 297–356.
- Fenoglio-Marc, L., J. Kusche, and M. Becker (2006). Mass variation in the Mediterranean Sea from GRACE and its validation by altimetry, steric and hydrology fields, *Geophys. Res. Lett.*, 33, L19606, doi:10.1029/2006GL026851.
- Güntner, A. (2008). Improvement of global hydrological models using GRACE data. *Surv. Geophys.* 29, p.375-397, doi:10.1007/s10712-008-9038-y.
- Guo, J., Y. Li, H. Deng, S. Xu, and J. Ning (2004). Green's function of the deformation of the earth as a result of atmospheric loading, *Geophys. J. Int.*, 159, 53–68.
- Guo, J.Y., X.J. Duan, C.K. Shum (2009). Non-isotropic Gaussian smoothing and leakage reduction for determining mass changes over land and ocean using GRACE data, accepted in *Geophys. J. Int.*
- Gutentag, E. D., F. J. Heimes, N. C. Krothe, R. R. Luckey and J. B. Weeks (1984). Geohydrology of the High Plains aquifer in parts of Colorado, Kansas, Nebraska, New Mexico, Oklahoma, South Dakota, Texas, and Wyoming, *U.S. Geol. Surv. Prof. Pap.*, 1400-B, 66 pp.

- 615 Han, S.C., C.K. Shum and C. Jekeli (2005). Improved estimation of terrestrial water storage changes from GRACE. *Geophys. Res. Lett.* 32:L07302. doi:10.1029/2005GL02238
- Han SC, C.K. Shum, C. Jekeli, C. Y. Kuo, C.R. Wilson and K.W. Seo (2005). Non-isotropic filtering of GRACE temporal gravity for geophysical signal enhancement. *Geophys J Int* 163:18–25. DOI 10.1111/j.1365-246X.2005.02756.x
- 620 Han, S.C., D.D. Rowlands, S.B. Luthcke and F.G. Lemoine (2008). Localized analysis of satellite tracking data for studying time-variable Earth's gravity field. *J. Geophys. Res* 113:B06401. doi:10.1029/2007JB005218
- Han, S.-C. and F.J. Simons (2008). Spatiospectral localization of global geopotential fields from the Gravity Recovery and Climate Experiment (GRACE) reveals the coseismic gravity change owing to the 2004 Sumatra-Andaman earthquake, *J. geophys. Res.*, 113, B01405, doi:10.1029/2007JB004927.
- 625 Han, S.-C., H. Kim, I.Y. Yeo, P. Yeh, T. Oki, K.W. Seo and D. Alsdorf (2009). Surface water storage in the Amazon inferred from measurements of inter-satellite distance change, *Geophys. Research Letters*, accepted.
- 630 Jekeli C (1981) Alternative methods to smooth the Earth's gravity field. Rep. 327, Dep. of Geod. and Sci. and Surv., Ohio State Univ
- Klees, R., E.A. Zapreeva, H.C. Winsemius and H.H.G. Savenije (2007). The bias in GRACE estimates of continental water storage Variations *Hydrol. Earth Syst. Sci.*, 11, 1227–1241, 2007
- 635 Klees, R., E.A. Revtova, B.C. Gunter, P. Ditmar, E. Oudman, H.C. Winsemius and H.H.G. Savenije (2008). The design of an optimal filter for monthly GRACE gravity models, *Geophys. J. Int.*, 175, 417-432
- Klees, R., X. Liu, T. Wittwer, B.C. Gunter, E. A. Revtova, R. Tenzer, P. Ditmar, H. C. Winsemius and H. H. G. Savenije (2008). A Comparison of Global and Regional GRACE Models for Land Hydrology. *Surv. Geophys.* 29(4-5), p.335-359, doi: 10.1007/s10712-008-9049-8
- 640 Kusche, J. (2007). Approximate decorrelation and non-isotropic smoothing of time-variable GRACE-type gravity field models. *J. Geod.*, 81, 733-749.
- Leblanc, M. J., P. Tregoning, G. Ramillien, S. O. Tweed and A. Fakes (2009). Basin-scale, integrated observations of the early 21st century multiyear drought in southeast Australia, *Water Resour. Res.*, 45, W04408, doi:10.1029/2008WR007333.
- 645 Lemoine, J.-M., S. Bruinsma, S. Loyer, R. Biancale, J.-C. Marty, F. Perosanz, and G. Balmino (2007). Temporal gravity field models inferred from GRACE data, *Adv. Space Res.*, 39, 1620 – 1629, doi:10.1016/j.asr.2007.03.062.
- Lettenmaier D.P. and J.S. Famiglietti (2006). Hydrology—water from on high. *Nature* 444(7119):562–563
- 650 McGuire, V. L. (2007). Water-level changes in the High Plains aquifer, predevelopment 482 to 2005 and 2003 to 2005, U.S. Geological Survey Scientific Investigation Report 483 2006-5324, 7 p.
- Ngo-Duc, T., K. Laval, G. Ramillien, J. Polcher and A. Cazenave (2007). Validation of the land water storage simulated by organising carbon and hydrology in dynamic ecosystems (ORCHIDEE) with gravity recovery and climate experiment (GRACE) data. *Water Res. Res.* 43, W04427. doi:10.1029/2006WR004941.
- 655 Niu, G.-Y. and Z.-L. Yang (2006). Assessing a land surface model's improvements with GRACE estimates. *Geophys. Res. Lett.* 33. doi:10.1029/2005GL025555.
- Niu, G.Y., Z.L. Yang, K. Mitchell, F. Chen, M.B. Ek, M. Barlage, L. Longuevergne and M. Tewari (2009). The community NOAA land surface model with multi-physics options, submitted to *Journal of Geophysical Research*.
- 660 Niu, G.Y., Yang, Z.L., Mitchell, K.E., Chen, F., Ek, M.B., Barlage, M., Longuevergne, L., Tewari, M. (2009) :The Community NOAA land surface model with multi-physics options : 2. Tests over Global River Basins, *Journal of Geophysical Research*, submitted.
- Pagiatakis, S. (1990). The response of a realistic Earth to ocean tide loading, *Geophys. J. Int.*, 103, 541–560.
- 665 Percival, D. B. and A. T. Walden (1993). *Spectral Analysis for Physical Applications, Multitaper and Conventional Univariate Techniques*, Cambridge Univ. Press, New York.

- Ramillien, G., F. Frappart, A. Cazenave and A. Güntner (2005). Time variations of land water storage from an inversion of 2 years of GRACE geoids. *Earth Planet Sci. Lett.* 235(1-2), 283-301.
- 670 Ramillien G, Frappart F, Güntner A, Ngo-Duc T, Cazenave A (2006) Mapping time variations of evapotranspiration rate from GRACE satellite gravimetry. *Water Resources Res* 42:W10403. doi: 10.1029/2005WR004331
- Ramillien, G., J.S. Famiglietti and J. Wahr (2008). Detection of continental hydrology and glaciology signals from GRACE: a review, *Surv. Geophys*, 29, 361-374, doi:10.1007/s10712-008-9048-9
- 675 Rodell, M. and J.S. Famiglietti (2002). The potential for satellite-based monitoring of groundwater storage changes using GRACE: the High Plains aquifer, Central US. *J. Hydrol.* 263(1-4), 245-256
- Rodell, M., P. R. Houser, U. Jambor, J. Gottschalck, K. Mitchell, C.-J. Meng, K. Arsenault, B. Cosgrove, J. Radakovich, M. Bosilovich, J. K. Entin, J. P. Walker, D. Lohmann, and D. Toll (2004a). The Global Land Data Assimilation System, *Bull. Amer. Meteor. Soc.*, 85 (3), 381–394.
- 680 Rodell M, Famiglietti JS, Chen J, Seneviratne SI, Viterbo P, Holl S, Wilson CR (2004b) Basin scale estimates of evapotranspiration using GRACE and other observation. *Geophys Res Lett* 31:L20504.doi:10.1029/2004GL020873
- Rodell, M., Velicogna, I. and Famiglietti, J.S. (2009). Satellite-based estimates of groundwater depletion in India. *Nature*, doi:10.1038/nature08238
- 685 Rowlands, D.D., S.B. Luthke, S.M. Klosko, F.G. Lemoine, D.S. Chinn, J.J. McCarthy, C.M. Cox, and O.B. Anderson (2005). Resolving mass flux at high spatial and temporal resolution using GRACE intersatellite measurements. *Geophys. Res. Lett.* 32:L04310. doi:10.1029/2004GL022386
- Sasgen, I., Z. Martinec, and K. Fleming (2006). Wiener optimal filtering of GRACE data, *Stud. Geophys. Geod.*, 50, 499–508.
- 690 Save, H.V. (2009). Using regularization for error Reduction in GRACE Gravity Estimation, PhD dissertation, the University of Texas at Austin, 113pp.
- Schmidt, R., F. Flechtner, U. Meyer, K.H. Neumayer, C. Dahle, R. König, and J. Kusche (2008). Hydrologic signals observed by the GRACE satellites. *Surv. Geoph.* doi:10.1007/s10712-008-9033-3.
- 695 Simons, F. J., F. A. Dahlen and M. A. Wieczorek (2006). Spatiospectral concentration on a sphere, *SIAM Rev.*, 48, 504 – 536, doi:10.1137/S0036144504445765.
- Simons, F.J., A. Dahlen (2008), Spherical Slepian functions and the polar gap in geodesy, *Geophys. J. Int.* 166, 1039-1061.
- 700 Seo, K.W. and C.R. Wilson (2005). Simulated estimation of hydrologic loads from GRACE, *J. Geod.*, 78, 442-456
- Seo, K.-W., C.R. Wilson, J.S. Famiglietti, J.L. Chen and Rodell, M. (2006). Terrestrial water mass load changes from gravity recovery and climate experiment (GRACE), *Water Resour. Res.*, 42, W05417, doi:10.1029/2005WR004255.
- 705 Seo, K.W., C.R. Wilson, J.L. Chen and Waliser, D.E. (2008). GRACE's spatial aliasing error, *Geophys. J. Int.*
- Slepian, D. (1978). Prolate spheroidal wave functions, Fourier analysis, and uncertainty - V: The discrete case. *Bell System Technical Journal*, 57, 1371–430.
- 710 Strassberg, G., B.R. Scanlon, and M. Rodell (2007). Comparison of seasonal terrestrial water storage variations from GRACE with groundwater-level measurements from the High Plains Aquifer (USA), *Geophys. Res. Lett.*, 34, L14402.
- Strassberg, G., B.R. Scanlon and D. Chambers (2009). Evaluation of Groundwater Storage Monitoring with the GRACE Satellite: Case Study High Plains Aquifer, Central USA, *Water Resour. Res*, 45, W05410, doi:10.1029/2008WR006892
- 715 Swenson, S. and J. Wahr (2002). Methods for inferring regional surface-mass anomalies from GRACE measurements of time-variable gravity. *J. Geophys. Res.*, 107(B9):2193. doi:10.1029/2001JB000576
- Swenson, S., J. Wahr, and P. C. D. Milly (2003). Estimated accuracies of regional water storage variations inferred from the Gravity Recovery and Climate Experiment (GRACE), *Water Resour. Res.*, 39, 1223, 2003.

- 720 Swenson, S. and J. Wahr (2006). Post-processing removal of correlated errors in GRACE data, *Geophys. Res. Lett.*, 33, L08 402, doi: 10.1029/2005GL025285
- Swenson, S. and J. Wahr (2007). Multi-sensor analysis of water storage variations of the Caspian Sea. *Geophys. Res. Lett.* 34,L16401, doi:10.1029/2007GL30733
- 725 Syed T.H., J.S. Famiglietti, M. Rodell, J. Chen and C.R. Wilson (2008a) Analysis of terrestrial water storage changes from GRACE and GLDAS. *Water Resour Res* 44:W02433. doi:10.1029/2006WR005779
- Syed TH, Famiglietti JS, Chambers D (2008b) GRACE-based estimates of terrestrial freshwater discharge from basin to continental scales. *J Hydrometeorol.* doi:10.1175/2008JHM993.1
- 730 Tang, Q., Gao, H., Yeh, P., Oki, T., Su, F. and Lettenmaier, D.P. Dynamics of terrestrial water storage change from observations and modeling, *J. Climate*, in review
- Tapley, B. D., S. Bettadpur, M. Watkins, and C. Reigber (2004). The gravity recovery and climate experiment: Mission overview and early results, *Geophys. Res. Lett.*, 31, L09607, doi:10.1029/2004GL019920.
- 735 Tapley, B.D., S. Bettadpur, J.C. Ries, P.F. Thompson and M.M. Watkins (2004). GRACE Measurements of Mass Variability in the Earth System, *Science*, 305(5683), 593-505. DOI: 10.1126/science.1099192
- Tiwari, V.M., J. Wahr and S. Swenson (2009). Dwindling groundwater resources in northern India from satellite gravity observations, *Geophys., Res., Lett.*, under press.
- 740 Thomson, D. J. (1982). Spectrum estimation and harmonic analysis, In *Proceedings of the IEEE*, 70, 1055–1096.
- Velicogna, I. and J. Wahr (2006). Measurements of time-variable gravity show mass loss in Antarctica, *Science*, 311, 1754–1756.
- 745 Wahr, J., M. Molenaar, and F. Bryan (1998). Time variability of the earth's gravity field: Hydrologic and oceanic effects and their possible detection using GRACE, *J. Geophys. Res.*, 103, 30 205–30 230, 1998.
- Wahr, J., S. Swenson, V. Zlotnicki and I. Velicogna (2004). Time-variable gravity from GRACE: First results, *Geophys. Res. Lett.*, 31, L11501, doi:10.1029/2004GL019779
- Wahr, J., S. Swenson, and I. Velicogna (2006). Accuracy of GRACE mass estimates. *Geophys. Res. Lett.* 33 (6), L06401. doi:10.1029/2005GL025305.
- 750 Wieczorek, M. A. and F. J. Simons (2005). Localized spectral analysis on the sphere, *Geophys. J. Int.*, 162, 655 –675, doi:10.1111/j.1365-246X.2005.02687.x.
- Werth, S., A. Güntner, S. Petrovic and R. Schmidt (2009): Integration of GRACE mass variations into a global hydrologic model, *Earth and Planetary Research Letters* 277(1-2), 166-173.
- 755 Zaitchik, B.F., M. Rodell and R.H. Reichle (2008). Assimilation of GRACE terrestrial water storage data into a land surface model: results for the Mississippi river basin. *J. Hydrometeorol.* 535–548

Figure captions

760 Figure 1: a) Outline of the High Plains aquifer (red), outline of the convex portion of the simple basin function (black). b) cross-section of basin function near latitude 41 (black). Basin function truncated to maximum degree $L_{\max} = 60$ (red). EBF stands for effective basin function.

765 Figure 2: Diagram synthesizing GRACE processing for basin-scale water storage estimate based on Level-2 Spherical Harmonics products

Figure 3: Transfer function of isotropic SH filters used in this study, a 300-km Gaussian filter and cosine taper from degrees 30 to 50.

770 Figure 4: Convergence on bias and leakage calculation with respect to grid size, for the HPA.

Figure 5: a) Comparison among several EBFs for the HPA at latitude N 40°. SH expansion maximum degree is 60. The Slepian EBF is the sum of the first two eigenvectors, with $L_h=50$. Differences between EBFs and the true basin $\hat{h} - h$ for Swenson's EBF (b) and Slepian EBF (c).

775 Figure 6: Spectrum characteristics of EBFs a) Swenson's EBF; b) Slepian EBF, both relative to the exact basin function; and c) RMS amplitude spectra of GRACE estimates as a function of SH degree after a 300-km Gaussian filter and bias correction are applied.

780 Figure 7: Leakage effect associated with various concentration methods after a cosine taper between degree 30 to 50 is applied, considering GLDAS-NOAH stored water variations (snow, vegetation and all soil moisture layers) as a-priori information.

785 Figure 8: Variation of reciprocal bias, concentration and final GRACE error estimate for the HPA as a function of the concentration method and the filtering method used (Gaussian or cosine taper as a function of the filter half-width). Destriping effect is shown for a truncated basin function only. Maximum degree for SH expansion is 60. Slepian function is built as the sum of the two first tapers, the bandwidth being limited by $L_h=50$. a) Concentration, b) mean value of EBF or reciprocal bias, c) CSR GRACE error after destriping algorithm is applied and leakage correction error; d) CSR total error; e) GRGS GRACE error and leakage correction error; and f) GRGS total error.

790 Figure 9: Comparison between GRACE-derived stored water variations for both CSR and GRGS solutions with water storage derived from ground-based measurements and GLDAS-NOAH model. Only GRACE measurement error is shown for clarity, leakage correction error is excluded (about 13 mm). SM and GW stands respectively for soil moisture and groundwater measurements.

6. Tables

| Method | Assumption |
|--|---|
| Same processing applied to GRACE and a-priori hydrological model | Fully trusts a-priori hydrological model relative amplitude between inside and outside the basin of interest (i.e. spatial patterns). Model error damped by $(h-\hat{h})$. Generally expressed as a single multiplicative coefficient |
| Equation (1) + Equation (2) | Partly trusts a-priori hydrological model relative amplitude over $(h-\hat{h})$. Model error damped by $(h-\hat{h})$. Bias and leakage contributions are calculated separately. Corrections expressed as time series. |
| Equation (4) + Equation (2) | No a-priori for water mass variations inside the area of interest except homogeneity, trusts a-priori hydrological model amplitude outside the area of interest. Model error damped by $(h-\hat{h})$. Required when the a-priori model does not fully model water storage variations (e.g. deep groundwater system) or when studying localized phenomena. Leakage correction expressed as time series. |

Table 1: synthesis of bias and leakage correction methods

800

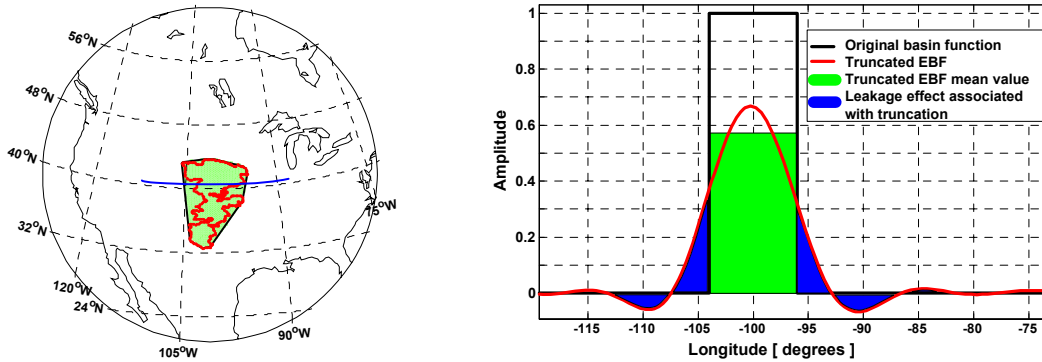
| | Processing applied | CSR solutions | GRGS solutions |
|---|---------------------------|------------------------------|------------------------------|
| HPa 450,000 km ² | Filter method | Cosine taper [30 50] | No filter |
| | Concentration method | Slepian EBF N=2 Lh=50 | Slepian EBF N=2 Lh=50 |
| | Concentration Δ | 0.60 | 0.66 |
| | Multiplicative factor k | 1.64 (1.23 using GLDAS-NOAH) | 1.45 (1.08 using GLDAS-NOAH) |
| | RMS error | 24 mm | 26 mm |
| Northern part of HPa, 210 000 km ² | Filter method | Cosine filter [40 60] | No filter |
| | Concentration method | Slepian EBF N=1 Lh=50 | Slepian EBF N=1 Lh=50 |
| | Concentration Δ | 0.60 | 0.60 |
| | Multiplicative factor k | 2.0 (1.32 using GLDAS-NOAH) | 1.66 (1.10 using GLDAS-NOAH) |
| | RMS error | 30 mm | 30 mm |
| Southern part of HPa, 240 000 km ² | Filter method | Cosine filter [30 50] | No filter |
| | Concentration method | Slepian EBF N=1 Lh=50 | Slepian EBF N=1, Lh=50 |
| | Concentration Δ | 0.55 | 0.58 |
| | Multiplicative factor k | 1.66 (1.29 using GLDAS-NOAH) | 1.47 (1.18 using GLDAS-NOAH) |
| | RMS error | 30 mm | 30 mm |

Table 2: Filtering and concentration applied for GRACE processing on the High Plains aquifer.

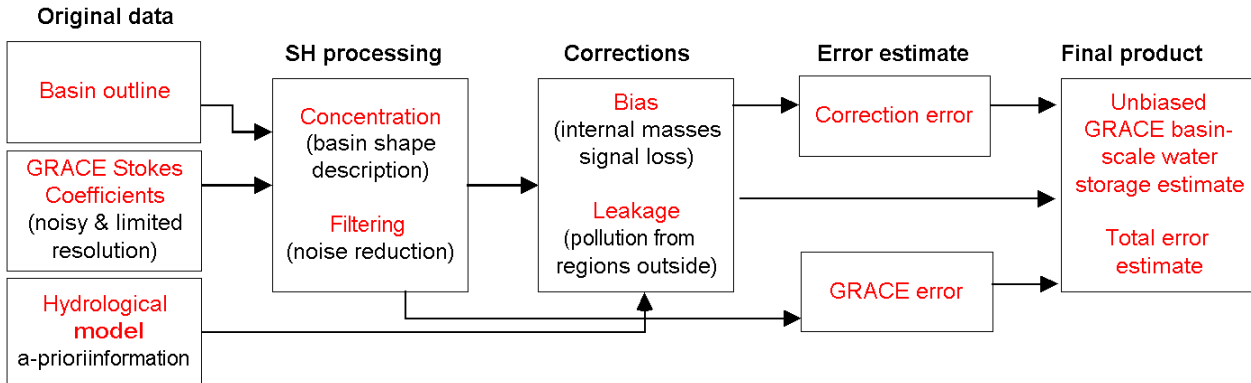
| | CSR | | | GRGS | | | |
|-----------|-----------|-----------|------|-----------|-----------|-----------|------|
| | Cor. 30 d | Cor. 90 d | Fact | Cor. 10 d | Cor. 30 d | Cor. 90 d | Fact |
| HPA | 0.80 | 0.87 | 1.18 | 0.70 | 0.71 | 0.77 | 1.12 |
| HPA north | 0.79 | 0.84 | 1.13 | 0.75 | 0.77 | 0.83 | 1.10 |
| HPA south | 0.80 | 0.88 | 1.12 | 0.75 | 0.78 | 0.87 | 1.12 |

805 Table 3: Correlation and amplitude factor between GRACE-derived water storage variations and soil moisture+groundwater analysis for several time scales. The amplitude factor is defined as the ratio between the standard deviations. Cor. stands for correlation and Fact. for amplification factor.

7. Figures



810 Figure 1: a) Outline of the High Plains aquifer (red), outline of the convex portion of the simple basin function (black). b) cross-section of basin function near latitude 41 (black). Basin function truncated to maximum degree $L_{\max} = 60$ (red). EBF stands for effective basin function.



815 Figure 2: Diagram synthesizing GRACE processing for basin-scale water storage estimate based on Level-2 Spherical Harmonics products

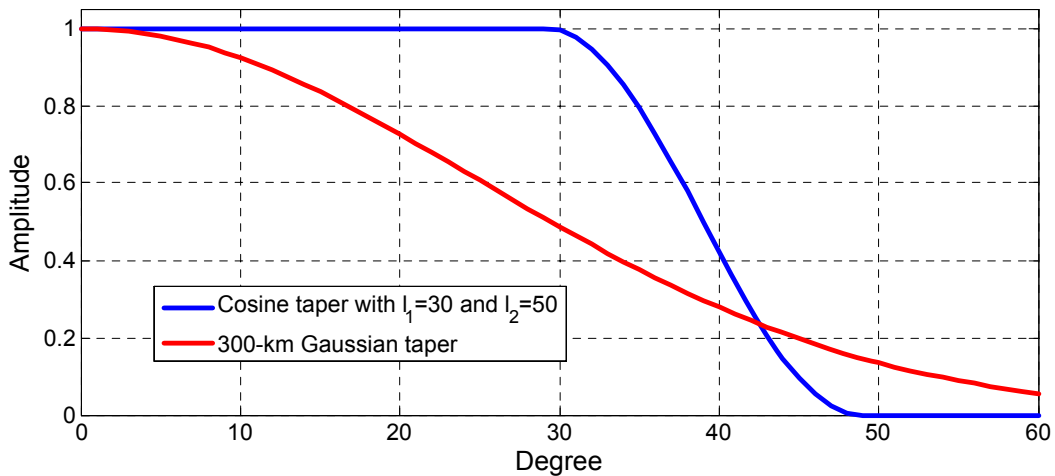
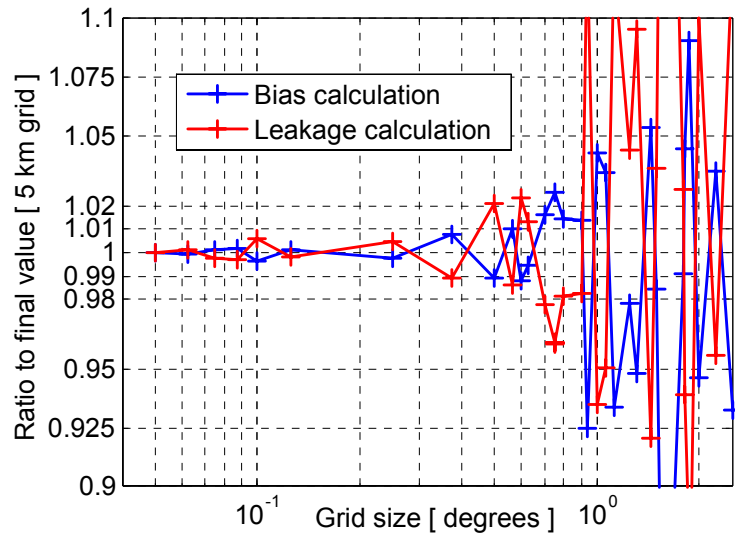
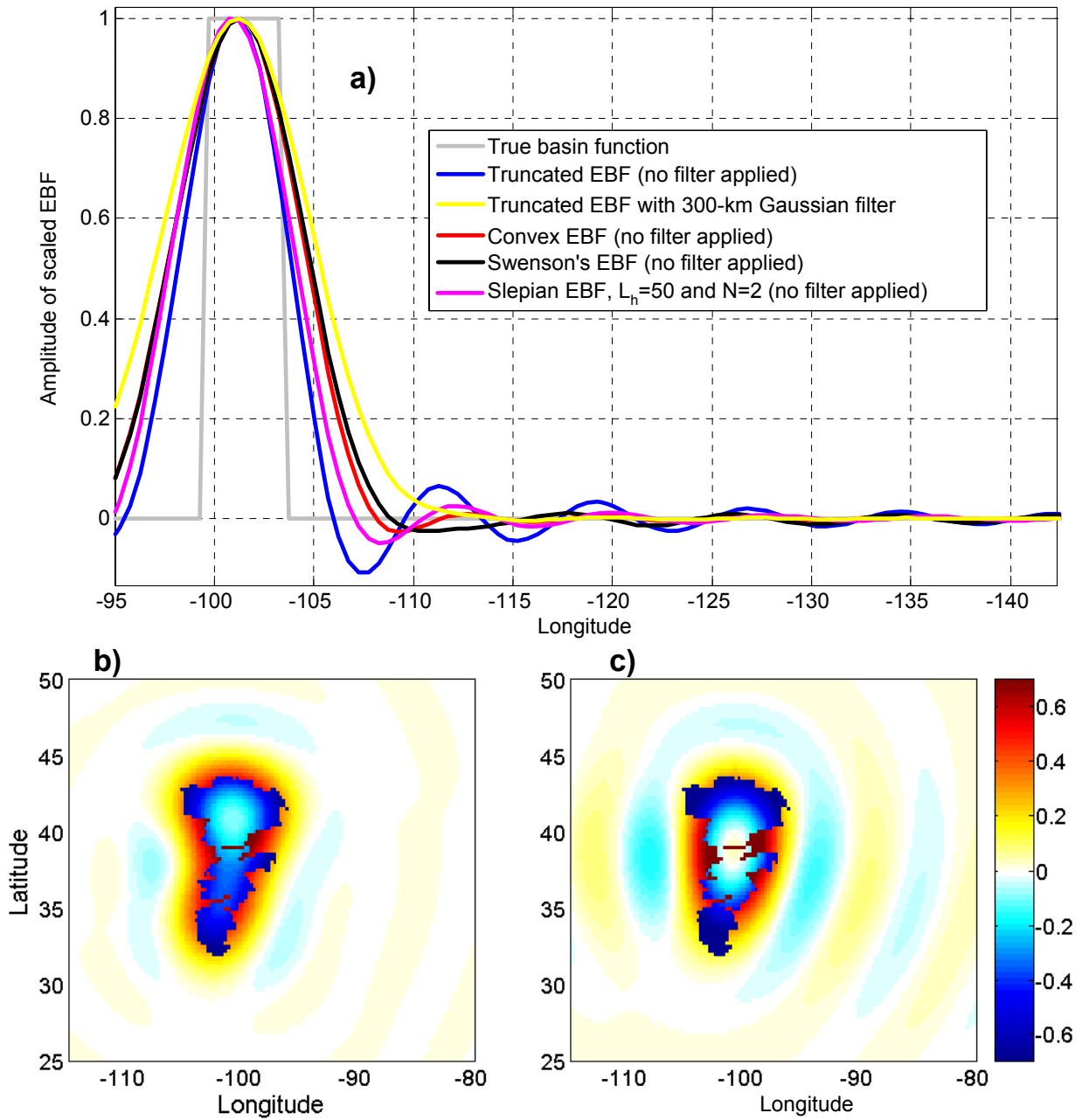


Figure 3: Transfer function of isotropic SH filters used in this study, a 300-km Gaussian filter and cosine taper from degrees 30 to 50.

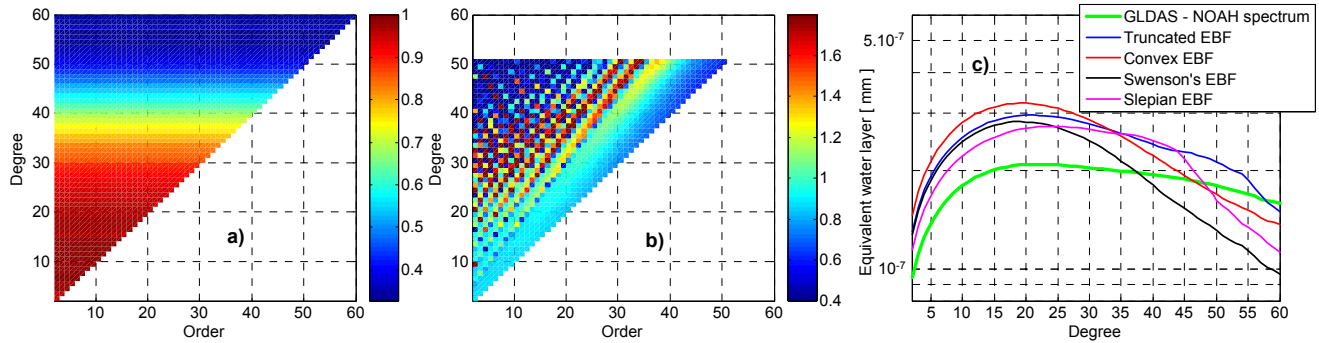


820

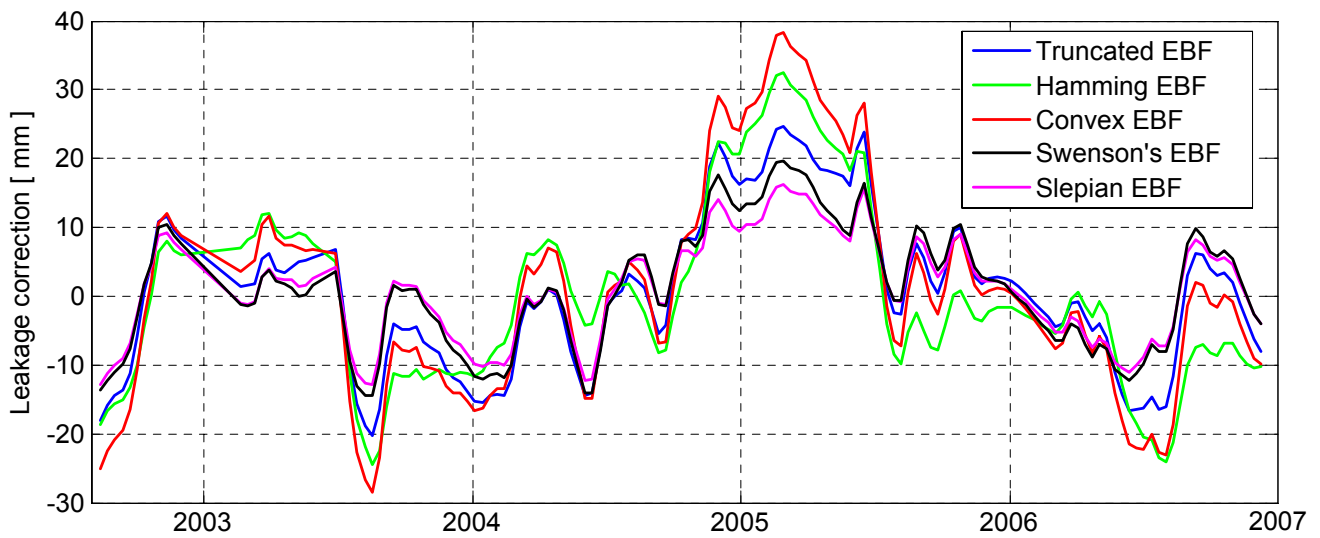
Figure 4: Convergence on bias and leakage calculation with respect to grid size, for the HPA.



825 Figure 5: a) Comparison among several EBFs for the HPA at latitude N 40°. SH expansion maximum degree is 60. The Slepian EBF is the sum of the first two eigenvectors, with $L_h=50$. Differences between EBFs and the true basin $\hat{h} - h$ for Swenson's EBF (b) and Slepian EBF (c).



830 Figure 6: Spectrum characteristics of EBFs a) Swenson's EBF; b) Slepian EBF, both relative to the exact basin function; and c) RMS amplitude spectra of GRACE estimates as a function of SH degree after a 300-km Gaussian filter and bias correction are applied.



835 Figure 7: Leakage effect associated with various concentration methods after a cosine taper between degree 30 to 50 is applied, considering GLDAS-NOAH stored water variations (snow, vegetation and all soil moisture layers) as a-priori information.

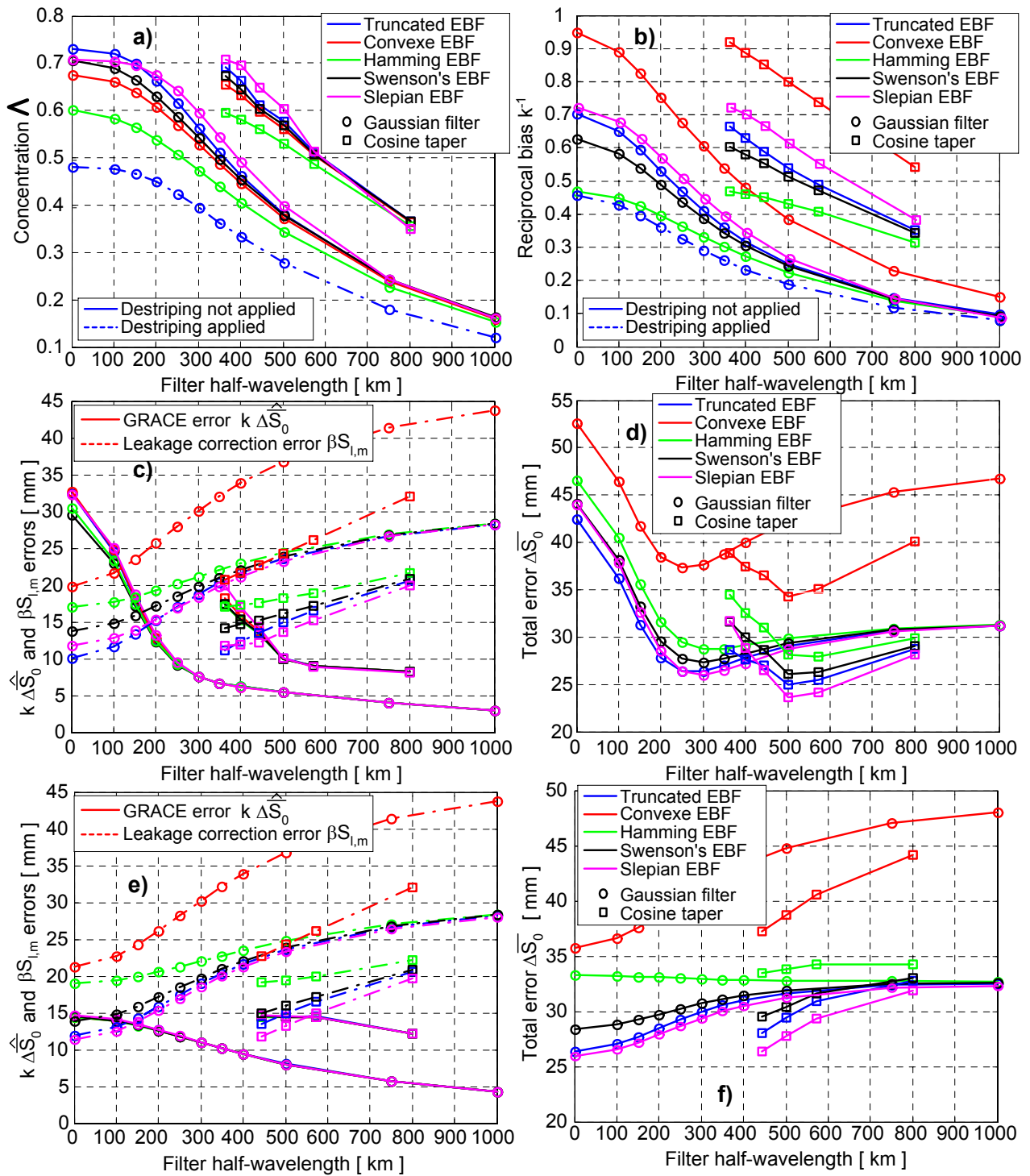
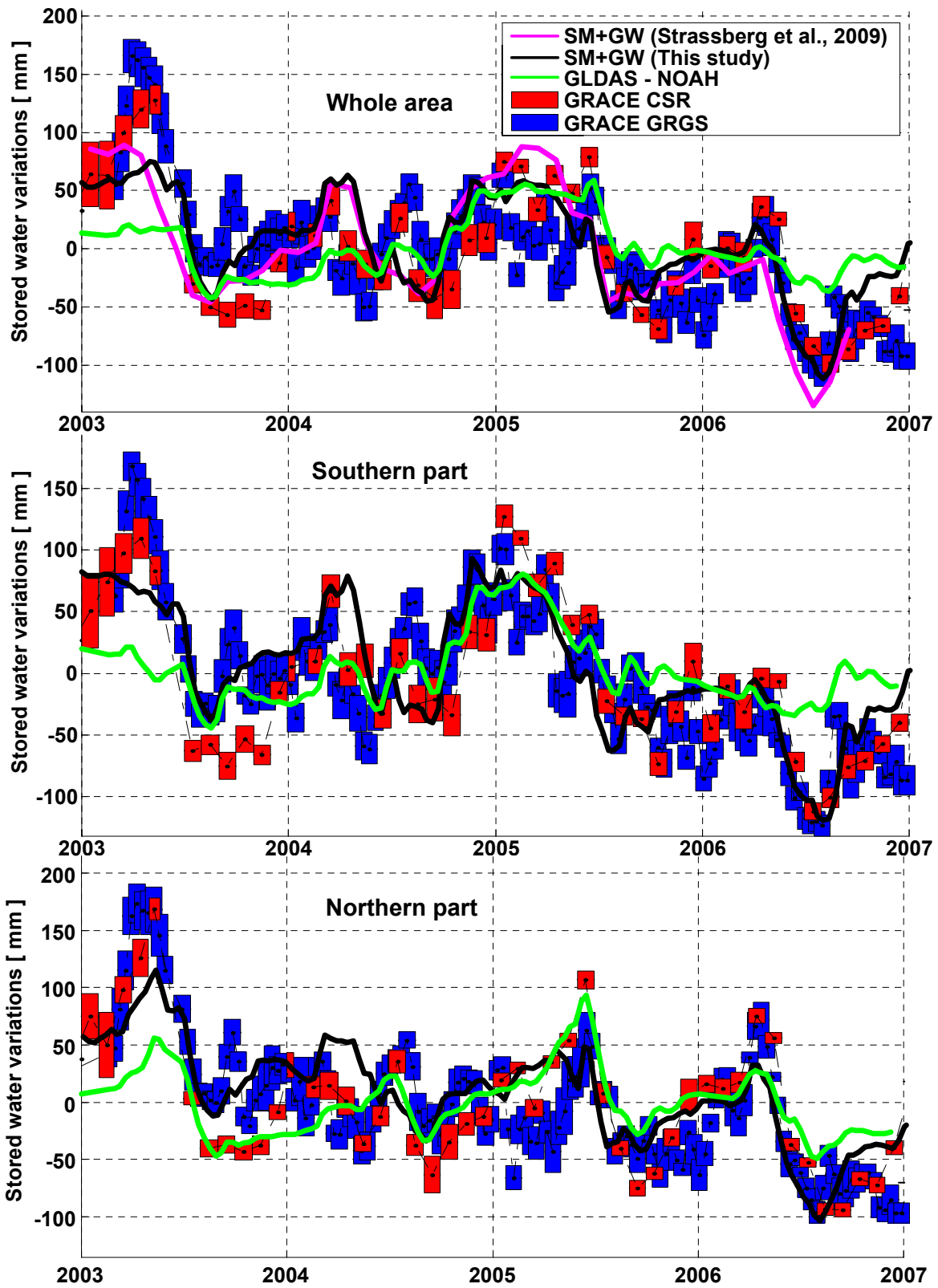


Figure 8: Variation of reciprocal bias, concentration and final GRACE error estimate for the HPA as a function of the concentration method and the filtering method used (Gaussian or cosine taper as a function of the filter half-width). Destripping effect is shown for a truncated basin function only. Maximum degree for SH expansion is 60. Slepian function is built as the sum of the two first tapers, the bandwidth being limited by $L_n=50$. a) Concentration, b) mean value of EBF or reciprocal bias, c) CSR GRACE error after destripping algorithm is applied and leakage correction error; d) CSR total error; e) GRGS GRACE error and leakage correction error; and f) GRGS total error.

840



845

Figure 9: Comparison between GRACE-derived stored water variations for both CSR and GRGS solutions with water storage derived from ground-based measurements and GLDAS-NOAH model. Only GRACE measurement error is shown for clarity, leakage correction error is excluded (about 13 mm). SM and GW stands respectively for soil moisture and groundwater measurements.